X-Band System Performance of the Very Large Array

J. S. Ulvestad
Tracking Systems and Applications Section

G. M. Resch
TDA Technology Development Office

W. D. Brundage
National Radio Astronomy Observatory
Socorro, New Mexico

The Very Large Array (VLA) is being equipped to receive telemetry from Voyager 2 during the Neptune encounter in 1989. Cryogenically cooled amplifiers are being installed on each of the 27 antennas. These amplifiers are currently a mix of field effect transistors (FETs) and high electron mobility transistors (HEMTs) and exhibit zenith system temperatures that range from 30 K to 52 K. We summarize the system temperatures and aperture efficiencies determined during the past year. The nominal values of the noise diode calibration are compared with derived values made under the assumption of a uniform atmosphere over the array. Gain values are determined from observations of unresolved radio sources whose flux densities are well known. The tests suggest that the completed VLA will have a ratio of gain to system temperature that is approximately 4.4 dB above that of a single 64-m antenna of the Deep Space Network.

I. Introduction

The Very Large Array (VLA) [1] in New Mexico will be arrayed with two or three Goldstone antennas during the Voyager encounter with Neptune and will support 21.6 kilobit/s telemetry from the spacecraft [2]. Initial plans called for equipping the VLA with cryogenically cooled FET amplifiers with an expected system temperature performance of 45–50 K at the Voyager downlink frequency of 8.42 GHz. During the planning phase of this implementation, the Deep Space Network (DSN) Advanced Systems Program and the National Radio Astronomy Observatory (NRAO) jointly began an effort with the General Electric Corporation and with Cornell University to examine the potential of a new type of transistor—a high electron mobility transistor (HEMT) [3] that might replace the FET and give better performance. This effort has been successful with the result that HEMTs are replacing the FETs and yielding roughly 15 K lower system temperatures at the zenith. The existing FET amplifiers will be replaced with HEMTs before the Neptune encounter.

The first 8.4 GHz amplifier (a FET) was installed in November 1984. There were two antennas with X-band capability until May 1986. Since then, X-band systems have been installed at the approximate rate of one every seven weeks. Through February 1987, there were seven antennas equipped with X-band capability, three with FET amplifiers and four with

HEMT amplifiers. As with the other VLA frequencies, each system consists of two intermediate frequency pairs. The right and left circularly polarized channels of one pair are designated "A" and "C," while those of the other pair are "B" and "D." Time on the array is allocated monthly in order to test system performance and operation with DSN telemetry receivers.

One of the tests that is often performed is a tip curve of all available X-band antennas in order to estimate the system temperatures including the atmospheric contribution. This is done for each antenna independently. Taken at face value, the tip curve data suggest unreasonably large variations of atmospheric temperature across the array, which implies inordinately large fluctuations of water vapor. We suspect that this result is due to two circumstances: (1) the *in situ* value of the calibration diode differs from its value determined in the laboratory; and (2) the actual value of the calibration diode varies slightly as a function of temperature and power supply current. We examine the nominal calibration of noise diodes on each antenna by assuming uniformity of the atmosphere and then derive a new value for the noise diode calibration level.

At various times, well-known radio sources are observed in order to estimate the antenna aperture efficiencies (i.e., the gain of the individual antennas). The ratio of the antenna gain to the system temperature, G/T, is an important parameter in the communications link performance and is derived for each antenna in operation by March 1987. In this article we summarize the results of the analysis of both the system temperature and aperture efficiency data from the past year.

II. System Temperature Data

The X-band configuration of the VLA antennas consists of dual amplifiers (one for each polarization) with a noise diode coupled to the input of each amplifier. The noise diodes can be switched on and off by one of the control computers and the output synchronously demodulated. Thus, the system is capable of being operated as a noise adding radiometer (NAR). The block diagram of the VLA electronics is shown in [1], and a description of the radiometric capability is given in [4]. The equivalent temperature of the noise diode is adjusted to be approximately 10 to 20 percent of the system temperature at the time each amplifier package is assembled and tested, but prior to installation on the antenna. This equivalent temperature of the noise diode is referred to as the "nominal value" and will vary slightly among the different amplifiers.

At X-band frequencies, the atmosphere radiates at an apparent temperature of several degrees; it can be used to calibrate the noise diode equivalent temperature much like a cold load. The technique that is used is called a "tip curve" and has both advantages and disadvantages as compared with the laboratory determination. The primary advantage is that the tip curve is done *in situ* on the antenna. The disadvantages are the following: (1) an independent measurement of atmospheric water vapor is needed; (2) it is necessary to calculate the emission of both water vapor and oxygen with high accuracy (if an absolute calibration is desired); (3) the atmosphere must be assumed to be plane-layered; and (4) the system temperature is dominated by radiation in the main beam of the antenna. These factors will be discussed as the analysis proceeds.

VLA operations provide the capability of running a procedure called TIPPER that drives all antennas in a sub-array to elevation angles of 60, 40, 30, 25, 20, 15, and 10 degrees. NAR data is taken at each of these elevation angles as the antennas tip toward the horizon at an azimuth of roughly 90 degrees, and then again at each of these elevations as the antennas return to zenith. The procedure takes approximately 15 minutes and provides 13 estimates (the 10 degree point is not repeated) of the system temperature (i.e., the brightness temperature of the sky). The tip curve data that we will consider in this article are summarized in Table 1.

A gating circuit is used to measure the "gated total power" level when the noise diode is off, V_{gtp}. This includes all contributions to the system temperature except for the automatically switching noise diode. This gated total power level is kept very near 3 volts by an automatic level control. The quantity V_{sd} is the voltage from the "synchronous detector," and is the observable during a tip curve. It represents the extra voltage from a square-law detector that is synchronized with the noise diode switch rate of 9.6 Hz. That is, this voltage shows the level of contribution of the noise diode in proportion to the nominal system temperature. The synchronous detector has a gain of 15 relative to the gated total power detector. Hence, if the noise diode contributes 10 percent of the system temperature, the ratio V_{sd}/V_{gtp} is $15 \times 0.1 = 1.5$. To compensate for this additional gain, the voltage at the gated total power detector is multiplied by 15 in the equation for the system temperature. Therefore, we have the following relation for the system temperature observed when the noise diode is off:

$$T_{\text{sys}} \propto \frac{15 V_{gtp}}{V_{sd}} \tag{1a}$$

A lower value of V_{sd} means that the noise diode contributes a smaller fraction of the system temperature, and hence that the overall system temperature is higher. Therefore, as an antenna

points to a lower elevation, the system temperature increases and V_{sd} decreases.

The nominal noise temperature contributed by the noise diode is T_{cal}, which is used to scale the voltage ratio in order to give the actual system temperature value. Hence,

$$T_{\text{sys}} \approx 15 T_{\text{cal}} \frac{V_{gtp}}{V_{sd}} \tag{1b}$$

The real expression for the system temperature at a VLA antenna is slightly more complex, because it also includes measured DC offsets of the two voltage detectors, V_{gtp_0} and V_{sd_0}. Thus, the final estimate of system temperature is given by the expression [5]

$$T_{\text{sys}} = 15 T_{\text{cal}} \frac{\left(V_{gtp} - V_{gtp_0}\right)}{\left(V_{sd} - V_{sd_0}\right)} \tag{1c}$$

Typically, V_{gtp} and the zero-level offsets, V_{gtp_0} and V_{sd_0}, change slowly and by very small fractional amounts. Operational procedure at the VLA is to measure these three values for each antenna intermediate frequency (IF) channel at roughly two-week intervals. Once determined, they are assumed constant and used in Eq. (1c) to calculate the system temperature. We will examine this assumption later, since changes in these values on time scales shorter than two weeks can lead to small errors in the system temperature or to apparent changes in the value of T_{cal}.

In the radiometry mode used for tip curves, an IF bandwidth of 50 MHz is used along with a minimum integration time of 1 s. Together with a T_{cal} value that is ~15 percent of T_{sys}, this gives an rms fluctuation level of approximately $10^{-3} \times T_{\text{sys}}$. That is comparable to the quantization level of the analog-to-digital converter, so that fluctuations occur in the least significant bit.

The system temperature looking at cold sky is

$$T_{\text{sys}} = T_{\text{rec}} + T_c e^{-\tau} + T_{\text{atm}} \tag{2}$$

Here, T_{rec} is the receiver temperature (in kelvins) referenced to the antenna aperture, T_c is the cosmic blackbody background temperature (2.8 K), T_{atm} is the temperature contribution by the atmosphere, and τ is the optical depth of the atmosphere in nepers. The atmospheric temperature is given by

$$T_{\text{atm}} = T_m \left(1 - e^{-\tau}\right) \tag{3}$$

where T_m is the mean radiating temperature of the atmosphere, in kelvins.

Note that the conventional definition of T_{rec} is referenced to the input of the first amplifier stage, whereas the definition made above includes losses and scattering in the antenna structure. If the atmosphere is plane layered then we can write,

$$\tau = \tau_0 \times \text{AM} \tag{4}$$

where τ_0 is the optical depth at the zenith (in nepers) and AM is the air mass (AM $\approx$ csc [elevation angle]). Given a set of data at elevation angles $E_1, E_2, \ldots, E_N$, the combination of Eqs. (1) and (2) gives a series of N equations that can be solved for some combination of the parameters T_{cal}, T_{rec}, and τ_0.

In the first part of the analysis we will assume that the values for T_{cal} are accurate for each system and use the tip curve data to solve for τ_0. Figure 1 shows the data from a typical tip curve with the system temperatures as calculated from Eq. (1) plotted versus the air mass. At the 8.4 GHz frequency the atmospheric opacity is typically small (i.e., $\tau \ll 1$), so the tip curve is linear with air mass. Note that the data are linear except for the point at 10 degree elevation (5.75 air masses).

The geometry of the feed and subreflector suggests that there is forward spillover that may be intercepting the land mask, which is typically greater than 0 degrees. At 10 degrees, this spillover picks up radiation from the earth at ~270 K and can contaminate the tip curve data even though the gain is reduced by 20 dB or more. For this reason we do not use any of the data from 10 degree elevation in the analysis. Figure 2 shows the residuals after we solved for the zenith opacity τ_0. We plot the observed system temperature minus that calculated from the fit, versus the air mass. The data at 10 degrees were not used in the fit, but are shown in the plot to emphasize that they are anomalous on almost all of the antennas and are very repeatable on a given antenna. When all of the tip curve residuals are averaged (except the 10 degree points), the rms at each elevation is on the order of 0.1 K.

After we have solved for the zenith opacity we can calculate the temperature contribution of the atmosphere from Eq. (3) if we know the mean radiating temperature of the atmosphere, T_m. Using a nominal value $T_m = 257$ K, we analyzed the tip curve data listed in Table 1. Note that we could have included T_m as a solved-for parameter. However, as shown in the appendix, T_{atm} is relatively insensitive to this quantity. Figure 3(a–j) shows the solved-for atmospheric temperature versus the antenna number where the "AB" and "CD" notation is the convention at the VLA to designate the two circular polarizations, right and left, respectively. Note

that antenna 10 came on line in February 1987 and is missing from the earlier tip curve data, and antenna 24 is missing from the 24 and 25 November data due to equipment problems.

Consider two aspects of these plots: first, the variation in the average level from one figure to the next; and second, the shape of each plot. Also note that although the average atmospheric temperature varies from day to day as we might expect, the general shape of the curve is remarkably consistent from month to month. The antenna-to-antenna variation is larger than we would expect from atmospheric fluctuations over the baselines in the array. The common element in this part of the analysis is the fact that we used the nominal values for T_{cal}. In the case of a perfectly stable, calibrated system and a stratified atmosphere, we would expect that the plots in Fig. 3 would be nearly flat; i.e., all antennas would report nearly the same value for T_{atm}. In reality, some variation would be expected due to (1) real variations in atmospheric water vapor or liquid (e.g., clouds or rain cells); (2) system noise; (3) changes in the offset calibration values; or (4) changes in the value of the noise diode calibration T_{cal}.

We might expect the average value of T_{atm} to vary from day to day due to slow changes in the atmosphere, changes dominated primarily by the water vapor content and liquid water in clouds. It is a relatively straightforward matter to solve the equation of radiative transfer and compute the apparent brightness temperature of the atmosphere at the frequency 8.4 GHz, given the amount and distribution of water vapor and oxygen. It is found that it takes 0.42 cm of precipitable water vapor to cause a 0.1 K change in T_{atm} at this frequency. This amount of water vapor is equivalent to a difference in propagation delay of 2.6 cm at the zenith over distances of a few kilometers. For a typical wind speed of 8 m/s, this would imply phase changes of three-fourths of a turn on time scales less than 500 sec. It is highly unlikely that the vapor over the array will differ by this amount, so we conclude that the assumption of constant atmosphere over the array is a good one.

As mentioned above, small changes in the offset data can cause systematic errors in the estimated brightness temperatures, or in our case changes in the derived values of T_{atm}. In order to estimate the size of these effects we used the tip curve data from the first tip curve on 26 October 1986 and reduced it using the offset data from 24 October 1986, 24 November 1986, 16 December 1986, 14 January 1987, and 19 February 1987. Table 2 summarizes the average as well as maximum positive and negative deviations from the first set of offset data. We see that although the average changes are quite small, there are "jumps" in the offset data that can cause relatively large changes in the solved-for parameters. The offset data for antennas 11AB and 11CD are listed in Table 3. The change in V_{sd_0} between 24 October and 24 November 1986 gives rise to changes of −0.131 K, −0.45 K, and −0.00052 neper in T_{atm}, T_{rec}, and τ_0, respectively. Similarly, the change in V_{gtp} between 14 January and 19 February 1987 causes changes of 0.144 K, 1.43 K, and 0.00057 neper in T_{atm}, T_{rec}, and τ_0. We conclude that, although the average values of these quantities are quite stable, variations on time scales of approximately two weeks or less in the offset data can lead to variations of ±0.15 K in the atmospheric temperaperature T_{atm}, ±1.4 K in the receiver temperature T_{rec}, and ±0.0006 in the zenith opacity τ_0 for a particular observation. If higher accuracy is required, calibration data should be sampled both before and after an observation. It seems unlikely that the offset data variations could give the repeatable signature shown in Fig. 3 over a six-month period.

The system noise can be estimated from the repeatability of the two tip curves taken on 26 October, about 1 hour apart, and comparing the solved-for parameters from each antenna channel. The average changes as well as maximum increases and decreases from the first to the second tip curve are listed in Table 4. We note that the absolute surface humidity values, as indicated by the temperature and dew point measurements, were 3.6 and 3.5 gm/m^3, respectively, for the start of the two tip curves, suggesting a stable atmosphere during the observations. We conclude that system noise can account for some of the small differences in Fig. 3(a–j) but cannot account for the large differences between antennas or for the repeatability of the signature.

If variations in the atmosphere, DC offset data, and system noise cannot account for the differences seen in Fig. 3(a–j), we are left with the possibility of variations in the calibration of the noise diode. The precise value of T_{cal} is determined in the laboratory for each individual amplifier by comparison with a cold load, using the technique described in [6]. The laboratory calibration of the diode equivalent temperature involves some intrinsic measurement uncertainty. This calibration may be different from the actual value on the antenna due to the slightly different impedances of the cold load and the antenna as seen by the amplifier. If we use the laboratory determination of T_{cal}, this would lead to a bias in the determination of system temperature. In addition, the noise diode is sensitive to the physical temperature of its surroundings (typically 0.01 dB per kelvin) and to small changes in the current through the device. Since the front-end area on the antenna is reasonably stable (±2 K), we might expect T_{cal} to change slowly around some nominal value due to temperature cycling. The temperature cycling is impossible to solve for without knowing the physical temperature variations in the front-end area. However, a potential bias in T_{cal} for each antenna can be extracted, at least in a relative sense.

In the second part of the analysis we adopt as the reference antenna 11AB. In this analysis, we force all antennas to "see" the same opacity as 11AB and solve for the value of T_{cal} for each tip curve. The 10 values for T_{cal} are then averaged to estimate the possible bias relative to antenna 11AB. Table 5 summarizes the nominal values of the noise diode calibration from the laboratory determination versus the solved-for values determined by the above procedure.

If we now use these new values of T_{cal} to reanalyze the tip curves, the variations in T_{atm} are much less pronounced. The dotted curves in Fig. 3(a–j) show the solved-for atmospheric temperature using these corrected T_{cal} values, and Table 6 summarizes the rms values obtained from using the nominal values of T_{cal} versus the solved-for values of T_{cal}. We see that the rms of T_{atm} is reduced by approximately a factor of two in this procedure and conclude that these new values of T_{cal} are more internally consistent than the nominal values. We have probably removed most of the bias term in T_{cal} that is due to differences in the laboratory value versus its *in situ* value. We have not reduced variations in T_{cal} around its average value, nor have we addressed its absolute value. Table 7 lists the zenith values for T_{sys} and T_{rec} derived using the new values of T_{cal}. Also, note that although the variation in T_{atm} from antenna to antenna is reduced, the rms is still more than we might reasonably expect from fluctuations in water vapor over the array.

III. Aperture Efficiency Measurements

No antenna does a perfect job of detecting the radiation that impinges on its primary surface. Some of the effects that reduce the efficiency of an antenna are diffraction effects, physical blockage by support structures, irregularities in the main and the subreflector shape, imperfect illumination, mechanical alignment of the feed and subreflector, subreflector focus, and pointing. The aperture efficiency is a measurement of the fraction of the radiation hitting the main reflecting surface that is actually detected; it is the ratio of the "effective" area of an antenna to its actual physical area. For monolithic radio telescopes operating at their primary observing frequencies, aperture efficiencies are typically 50–70 percent. The efficiency also tends to be reduced when observations are made at low elevation angles because of increased deformation of the telescope surfaces.

The VLA antennas were designed to work well at frequencies up to 22 GHz. Therefore, good aperture efficiencies should be expected at 8.4 GHz if the new X-band systems are designed and installed properly. Measurements of the aperture efficiencies of the antennas with X-band systems thus serve to verify the overall design and ensure that the hardware is installed properly on the telescopes.

Aperture efficiencies are typically found by measuring the antenna temperatures given by observations of radio sources with known flux densities. The effective area of a telescope is given by the formula $A_e = 2kT_{ant}/S$, where k is Boltzmann's constant, T_{ant} is the antenna temperature contributed by the radio source, and S is the radio source flux density. Since the effective area is simply the aperture efficiency ϵ multiplied by the physical area A_p, the efficiency is then given by the equation,

$$\epsilon = \frac{2kT_{ant}}{SA_p} \tag{5}$$

Frequently, this expression is rearranged to give an expression for the overall sensitivity of a telescope,

$$\frac{T_{ant}}{S} = \frac{\epsilon A_p}{2k} = \frac{A_e}{2k} \tag{6}$$

In normal radio astronomy usage, this sensitivity is expressed in kelvins per jansky, where the jansky is the unit of radio flux density and is defined to be equal to 10^{-26} W/m^2/Hz.

The antenna temperature is simply the difference between the system temperature measurements on and off source. The system temperature of a VLA antenna is measured using the NAR and calculated using the expression for T_{sys} given in the previous section. Therefore, the final expression for the aperture efficiency (dimensionless) of a VLA antenna becomes:

$$\epsilon = \frac{30kT_{cal}\left(V_{gtp} - V_{gtp_0}\right)}{SA_p}\left[\frac{1}{\left(V_{sd} - V_{sd_0}\right)_{on}} - \frac{1}{\left(V_{sd} - V_{sd_0}\right)_{off}}\right] \tag{7}$$

The VLA has a standard observing mode which can be used to measure aperture efficiencies. This mode is somewhat more elaborate than just making simple measurements on and off source. Instead, the antennas point at a specified source position and at four points separated from that position by a distance equal to the nominal half-power half-width of the beam. Two points are offset by plus or minus half a beamwidth in elevation, while the other two are offset by plus or minus half a beamwidth in azimuth. Interleaved among the "on-source" and "half-power-point" measurements are observations that are made 5 beamwidths off source in azimuth. At the 8.4 GHz operating frequency the antenna has a half-power beamwidth of 90 millidegrees and the peak pointing residuals are typically 2 to 3 millidegrees, so the effective pointing loss is less than 1 percent. However, there is a known beam squint between the two polarizations that causes point-

ing offsets of 5 millidegrees in azimuth and 1.5 millidegrees in elevation at 8.4 GHz. We have chosen to optimize the pointing for both polarizations simultaneously so as to use a single set of pointing offsets. This results in measured antenna efficiencies that are systematically 1–2 percent lower than theoretically possible.

The procedure for determining the aperture efficiency via measurements of a given source is straightforward. The fringe amplitude on a strong point source is measured relative to the standard flux density calibrator 3C286, whose flux density is assumed to be 5.20 Jy at X band. This gives the value for S to be used in the efficiency formula. The observing mode described above is used to measure the synchronous detector voltage both on and off source. If necessary, the measurements made at the half-power points are used to correct the on-source measurements for possible pointing errors. Such corrections are not made if the pointing has been checked prior to the observing session and found to be adequate. Then, the measured numbers are used to calculate the efficiency for each polarization of each available antenna. When time permits, measurements on several different sources are made consecutively.

Aperture efficiency measurements have been made periodically since the beginning of 1986. Since only two X-band antennas were available until about mid-1986, the histories on other antennas cover no more than nine months. Table 8 summarizes the results for each antenna measured to date, using the solved-for values of T_{cal}. Elevation-angle dependence is ignored in this table. Right and left circularly polarized data are distinguished, and the rms error is also given. Quoted errors are statistical only, and do not take possible systematic effects into account. One IF pair for antenna 11 (the "BD" pair) is not included, because it consistently gives abnormally high efficiency values, presumably due to some instrumental problem that has not yet been tracked down. Values for antenna 10 should be considered preliminary, since it was recently brought on line and was measured only via observations of three different radio sources in February 1987. Note that the efficiency for antenna 20 is considerably lower than that for the other antennas. Antenna 20 was the first VLA antenna to be equipped at X band; it uses a nonstandard feed and receiver rather than the production models that were installed on the other antennas. The preliminary feed design is thought to account for the low efficiency and will be swapped for a production model prior to the encounter.

Summaries for various combinations of data are given at the bottom of Table 8. For reasons stated above, no data from antenna 20 are included in the summaries. The agreement among the other antennas is fairly good, although there are some discrepancies such as the apparently low efficiency for the left circularly polarized feed of antenna 24.

The three radio sources used most often for aperture efficiency measurements were 3C273, 3C279, and 3C345. In general, 3C273 gave higher aperture efficiencies than the other two sources. This may be caused by the fact that 3C273 is about three times stronger at X band than are the other two sources. It contributes slightly more than 3 K, or about 10 percent for a HEMT-equipped antenna, to the total system temperature. The other two sources contribute only about 3 percent to the system temperature. Detector nonlinearities or differing signal-to-noise ratios may account for the apparent difference in aperture efficiency. No other sources have been measured often enough to confirm that the possible effect is actually dependent on source strength. Since 3C273 and 3C279 are much further south than 3C345, they were typically measured at lower elevations. The data listed in Table 8 were taken at elevation angles between 30 and 45 degrees and are not sufficient to determine potential elevation angle dependence.

Including the possible systematic errors caused by noise diode variations and by measurements of different sources, the best estimate for the aperture efficiencies of the VLA X-band systems is 0.62 ± 0.03 at elevations of ~40 degrees. The antenna sensitivities are then computed to be 0.110 ± 0.005 K/Jy.

IV. Ratios of Gain to System Temperature

The overall figure of merit of an antenna is determined by a combination of its noise level and its gain. For a VLA antenna at X band, the ratio of gain to system temperature (hereafter G/T) is given by

$$G/T = 4.859 \times 10^6 \frac{\epsilon}{T_{sys}} \tag{8}$$

The numerical factor in this equation is derived from the definition of the gain, $G = 4\pi A_e/\lambda^2$ (e.g., [7]). The symbol λ represents the observing wavelength.

Note that the value of G/T depends only on the aperture efficiency and system temperature of an antenna of a given physical size. The preceding sections have described the separate calculations of the aperture efficiencies and system temperatures. One of the major uncertainties in the determination of each quantity individually is the possible error or variation in the effective temperature of the noise diode, T_{cal}. However, as shown by Eqs. (1) and (7), both aperture efficiency and system temperature values are directly proportional to the assumed temperature of the noise diode. There-

fore, in the evaluation of Eq. (8), the assumed value of T_{cal} divides out and is removed as a source of error in the determination of antenna figure of merit.

The values of G/T for all of the VLA antennas equipped at X band are shown in Table 9. For four HEMT-equipped antennas (numbers 3, 10, 11, and 24), the weighted mean value of G/T is found to be 9.40×10^4 K^{-1} at the zenith, with an rms of 6.0×10^3 K^{-1}. The value of G/T at 30 degree elevation is also of importance; since the Voyager spacecraft is at a southerly declination, its maximum elevation at the VLA during the Neptune encounter phase will be ~34 degrees. Assuming an atmospheric temperature of 2.7 K per air mass, we find $G/T = 8.65 \times 10^4$ K^{-1} at 30 degree elevation. By comparison, we note that the most sensitive VLA frequency prior to the X-band installation was 5.0 GHz (C band). At that band, the VLA antennas have typical system temperatures of 50 K and aperture efficiencies of 0.65 at zenith. Using these values and the wavelength of X band, we calculate $G/T = 6.32 \times 10^4$ K^{-1} at zenith. Thus, the VLA antennas have a typical G/T at X band that is about 50 percent higher than would be expected if their overall performance were the same as at C band. This is consistent with the fact that the antennas that were initially equipped with FETs at X band give measured values of G/T that are near 6×10^4 K^{-1}.

At 30 degree elevation, the sum of 27 VLA antennas (assuming all HEMT amplifiers) with zero relative phase would give a net G/T of 2.34×10^6 K^{-1}, or 63.7 dB/K. Including a 1.0 dB loss because of the 3-level quantization and the periodic data gap at the VLA, the final estimate of G/T is then 62.7 dB/K. By comparison, a 64-m antenna of the Deep Space Network (DSN), assumed here to have a 50 percent aperture efficiency and a system temperature of 25 K at 30 degree elevation, would have G/T = 58.0 dB/K. Therefore, the performance of the individual antennas at the VLA predicts that the array of 27 antennas will give an overall enhancement of 4.7 dB, or a factor of 2.9, over the G/T of a single 64-m DSN antenna. There will likely be a modest signal loss of 0.2 to 0.3 dB because the 27 VLA antennas will have nonzero relative phases caused by system noise and by imperfectly corrected tropospheric disturbances. Thus the net improvement afforded by the VLA will be about 4.4 dB relative to a single 64-m antenna, making the VLA "worth" approximately 2.75 64-m antennas.

V. Summary

The system temperatures, aperture efficiencies, and gain to system temperature ratio for the 7 VLA antennas that were equipped with X-band amplifiers as of March 1987 have been measured. An internally consistent set of system temperature calibrations was derived referenced to antenna 11 and listed in Table 7. Aperture efficiencies, as summarized in Table 8, were derived by observing several strong radio sources whose flux densities were measured relative to the calibration source 3C286. The G/T ratio for the HEMT-equipped antennas was found to be 9.40×10^4 K^{-1} at the zenith. The fully phased VLA is predicted to have a G/T value that is 4.4 dB above that of a single 64-m DSN antenna.

References

[1] P. J. Napier, A. R. Thompson, and R. D. Ekers, "The Very Large Array: Design and Performance of a Modern Synthesis Radio Telescope," *Proc. IEEE*, vol. 71, pp. 1295–1320, 1983.

[2] J. W. Layland and D. W. Brown, "Planning for the VLA/DSN Arrayed Support to the Voyager at Neptune," *TDA Progress Report 42-82*, vol. April–June 1985, Jet Propulsion Laboratory, Pasadena, California, pp. 125–135, August 15, 1985.

[3] S. M. Petty, "Microwave Devices," in *Low-Temperature Devices*, R. K. Kirshman (ed.), New York: IEEE Press, 1986, pp. 358–363.

[4] A. R. Thompson, *An Introduction to the VLA Electronics System*, VLA Technical Report No. 29, Charlottesville, Virginia: NRAO, March 1977.

[5] "GTTSYS–System Temperature Entry Into Gain Table," in *VLA Observers' Reference Manual*, Socorro, New Mexico: NRAO, 1987.

[6] S. Weinreb, *Calibration of HP-346B Noise Sources at 1.3–1.7 GHz*, NRAO Electronics Division Technical Note No. 111, Charlottesville, Virginia: NRAO, July 1982.

[7] J. D. Kraus, *Radio Astronomy*, New York: McGraw-Hill, pp. 212–214, 1966.

[8] G. M. Resch, "Inversion Algorithms for Water Vapor Radiometers Operating at 20.7 and 31.4 GHz," *TDA Progress Report 42-76*, vol. October–December 1983, Jet Propulsion Laboratory, Pasadena, California, pp. 12–26, February 15, 1984.

Table 1. Summary of tip curve observations*

Date	Time	Temperature	Dew point	Remarks
26 Oct. 1986	1000	9.0	-3.9	Clear and dry
26 Oct. 1986	1050	11.9	-4.6	Clear and dry
27 Oct. 1986	1340	16.3	-5.5	Clear and dry
24 Nov. 1986	1110	2.7	-9.2	Clear
25 Nov. 1986	1350	9.8	-4.1	Clear
16 Dec. 1986	1030	3.2	1.7	Heavy overcast, drizzle
13 Jan. 1987	0800	-9.0	-10.9	Clear
19 Feb. 1987	1200	-3.9	-7.3	Cloudy, fog, snow on dishes
27 Feb. 1987	0140	-4.4	-7.5	Clear and calm
1 Mar. 1987	0140	-8.0	-9.4	Clear and calm

*Time is the start in mountain standard time zone; surface temperature and dew point near the array center are given in degrees Celsius.

Table 2. Changes in solved-for parameters due to changes in the offset data

Parameter	Average change	Maximum increase	Maximum decrease
T_{atm} (K)	0.0007	0.144	-0.131
T_{rec} (K)	0.09	1.43	-0.45
Opacity (nepers)	$<10^{-5}$	0.00057	-0.00052

Table 3. Summary of offset data (in volts) for antennas 11AB and 11CD

11AB				11CD			
Date	V_{gtp_0}	V_{gtp}	V_{sd_0}	Date	V_{gtp_0}	V_{gtp}	V_{sd_0}
24 Oct. 1986	-0.08	3.01	-0.094	24 Oct. 1986	-0.03	3.02	0.005
13 Nov. 1986	-0.08	3.00	0.041	13 Nov. 1986	-0.03	3.02	0.004
10 Dec. 1986	-0.04	2.99	0.074	10 Dec. 1986	-0.03	3.02	0.005
14 Jan. 1987	-0.03	3.02	-0.015	14 Jan. 1987	-0.04	3.06	-0.004
19 Feb. 1987	-0.03	3.02	0.018	19 Feb. 1987	-0.04	2.85	0.008

Table 4. Changes of solved-for parameters from successive tip curves obtained on 26 October 1986

Parameter	Average change	Maximum increase	Maximum decrease
T_{sys} (K)	−0.13	0.06	−0.27
T_{atm} (K)	−0.0084	0.062	−0.082
T_{rec} (K)	−0.12	0.14	−0.33
τ_0 (neper)	0.00003	0.00025	−0.0003

Table 5. Nominal and solved-for values of the noise diode value T_{cal} (in kelvins)*

Antenna	T_{cal}		rms	Ratio†
	Nominal	Solved-for		
3AB	4.20	4.71	0.24	0.892
3CD	4.33	4.70	0.26	0.922
10AB	4.33	4.68	0.08	0.925
10CD	4.50	4.59	0.10	0.980
11AB	4.03	4.03	0.001	0.9999
11CD	3.94	3.92	0.17	1.004
20AB	5.00	4.91	0.21	1.019
20CD	4.20	4.69	0.22	0.896
21AB	3.70	3.70	0.16	1.001
21CD	4.00	3.85	0.14	1.039
24AB	4.32	4.48	0.17	0.965
24CD	4.21	4.02	0.14	1.047
25AB	4.07	4.22	0.25	0.965
25CD	3.99	4.17	0.28	0.957

*Antenna 11AB was used as the reference for the opacity, and T_{cal} was computed on all other channels to give the same opacity for each tip curve.

†Ratios are those of the nominal values to the solved-for values of the noise diode temperatures.

Table 6. Comparison of the atmospheric temperature (in kelvins) derived from tip curve data, using two different values of T_{cal} for each antenna IF*

Date	Before correction		After correction	
	T_{atm}	rms	T_{atm}	rms
Oct. 26 (a)	2.66	0.13	2.73	0.05
Oct. 26 (b)	2.67	0.11	2.74	0.05
Oct. 27	2.70	0.12	2.77	0.06
Nov. 24	2.58	0.22	2.64	0.13
Nov. 25	2.57	0.22	2.65	0.14
Dec. 16	2.81	0.24	2.90	0.16
Jan. 13	2.59	0.13	2.67	0.04
Feb. 19	2.89	0.16	2.97	0.14
Feb. 27	2.62	0.13	2.70	0.06
Mar. 1	2.57	0.13	2.64	0.05

*Nominal values of T_{cal} were used first and then corrected by taking antenna 11AB as a reference.

Table 7. Average zenith system temperature and receiver temperature (K) for each antenna, as found using the solved-for values of T_{cal}

Antenna	T_{sys}	rms	T_{rec}	rms
3AB	33.1	1.4	27.6	1.4
3CD	34.8	1.2	29.3	1.3
10AB	37.5	1.4	32.0	1.3
10CD	34.8	1.2	29.2	1.1
11AB	31.1	0.5	25.6	0.4
11CD	29.9	0.8	24.4	0.7
20AB	44.7	0.5	39.2	0.5
20CD	49.5	0.5	44.0	0.4
21AB	46.5	0.6	41.0	0.6
21CD	47.8	0.8	42.3	0.7
24AB	27.5	1.0	22.0	1.0
24CD	29.4	1.0	23.9	1.0
25AB	51.7	1.2	46.1	1.2
25CD	51.7	1.2	46.2	1.2

Table 8. Aperture efficiency measurements of VLA antennas

Antenna	Receiver	RCP		LCP		Total	
		ϵ	rms	ϵ	rms	ϵ	rms
3	HEMT	0.659	0.061	0.661	0.046	0.660	0.052
10	HEMT	0.636	0.031	0.631	0.033	0.634	0.032
11AC	HEMT	0.621	0.029	0.606	0.031	0.614	0.030
20	FET	0.545	0.047	0.570	0.036	0.561	0.040
21	FET	0.603	0.048	0.599	0.044	0.601	0.046
24	HEMT	0.614	0.028	0.567	0.042	0.600	0.033
25	FET	0.614	0.061	0.619	0.053	0.617	0.057
Weighted mean (no 20)		0.623	0.037	0.613	0.039	0.618	0.038
Weighted mean (HEMT)		0.625	0.033	0.615	0.037	0.621	0.035
Weighted mean (3C273)		0.651	0.041	0.637	0.033	0.643	0.036
Weighted mean (3C345)		0.607	0.036	0.591	0.042	0.600	0.039
Weighted mean (3C279)		0.620	0.045	0.617	0.049	0.619	0.047

Average source fluxes:

S(3C273) = 31 Jy
S(3C345) = 11 Jy
S(3C279) = 10 Jy

Table 9. List of G/T values (units of 10^4/K)

Antenna	Receiver	RCP		LCP		Total	
		G/T	rms	G/T	rms	G/T	rms
3	HEMT	9.67	0.98	9.23	0.72	9.38	0.82
10	HEMT	8.24	0.51	8.81	0.55	8.50	0.53
11AC	HEMT	9.70	0.48	9.85	0.57	9.76	0.52
20	FET	5.92	0.51	5.60	0.36	5.71	0.42
21	FET	6.30	0.51	6.09	0.46	6.18	0.48
24	HEMT	10.85	0.63	9.37	0.76	10.25	0.69
25	FET	5.77	0.59	5.82	0.52	5.80	0.55
Weighted mean (HEMT)		9.47	0.58	9.31	0.63	9.40	0.60
Weighted mean (FET, no 20)		6.07	0.55	5.97	0.49	6.01	0.52

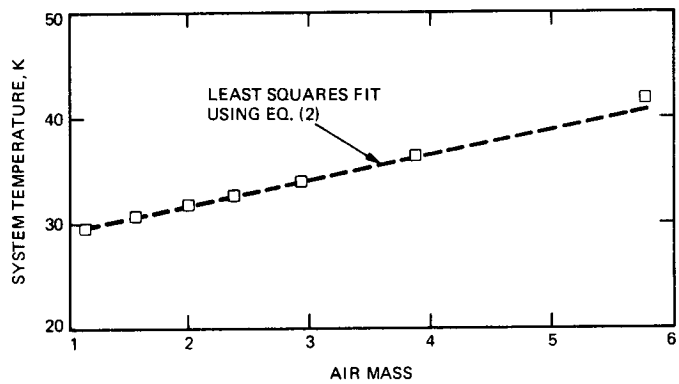

Fig. 1. Data plotted from antenna 3, channel AB, showing the total system temperature versus the air mass, illustrating a typical tip curve. Note that the datum at 10 degree elevation (*AM* = 5.8) is plotted but not used in the fitting procedure.

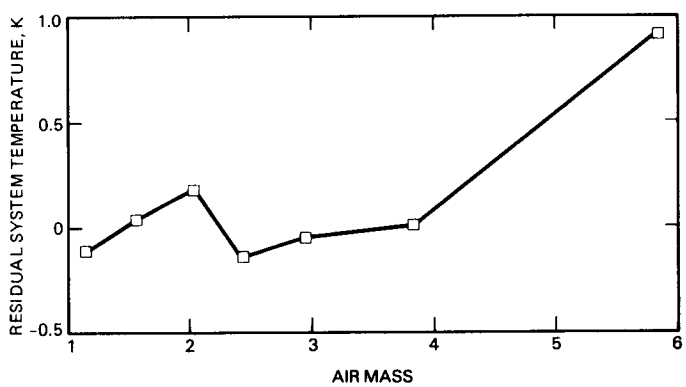

Fig. 2. Plot of the residuals from Fig. 1. Neglecting the point at *AM* = 5.8, the residuals are typically less than 0.2 K.

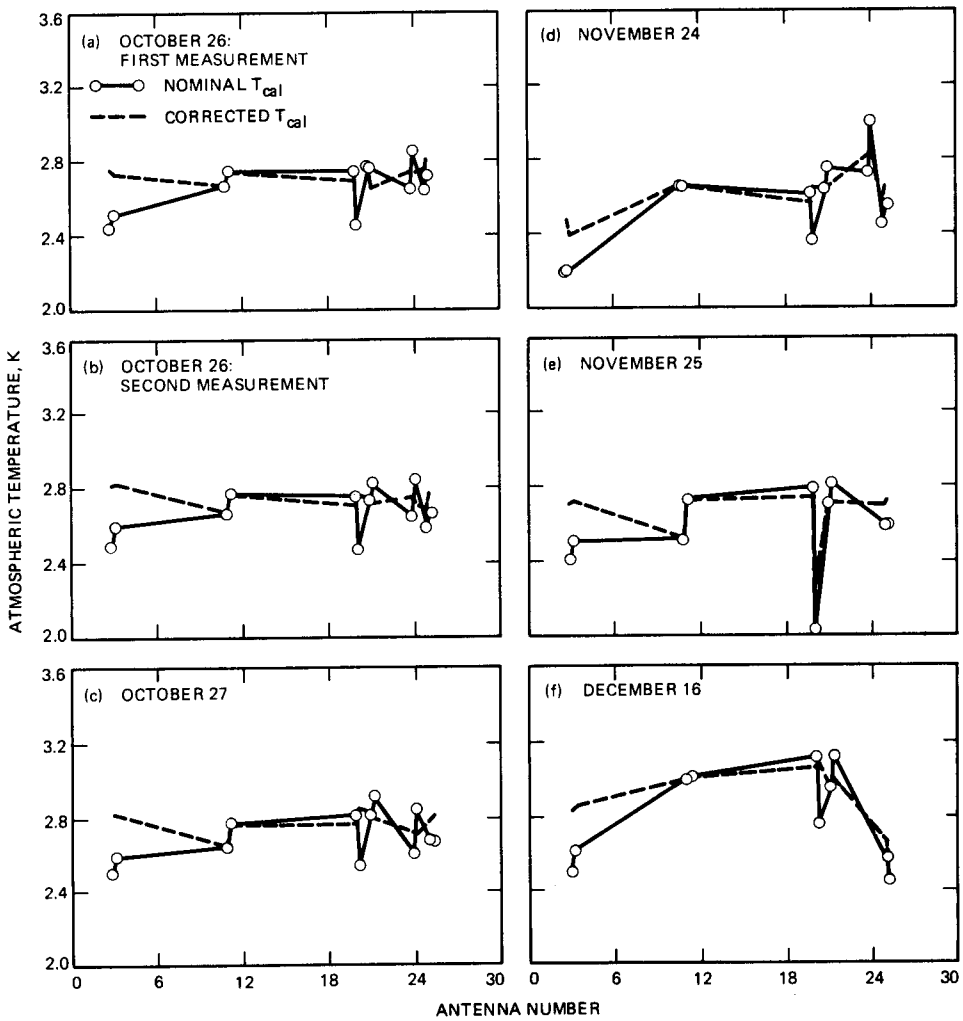

Fig. 3. For each of the tip curves listed in Table 1, these plots show the atmospheric temperature solved for from Eqs. (1) and (2), versus the antenna number. The solid line connects the data points indicating the solution using the nominal values of T_{cal}. The dotted lines indicate the values of T_{atm} using the solved-for values of T_{cal} listed in Table 5. Note the reduced variation in the dotted lines when compared to the solid lines.

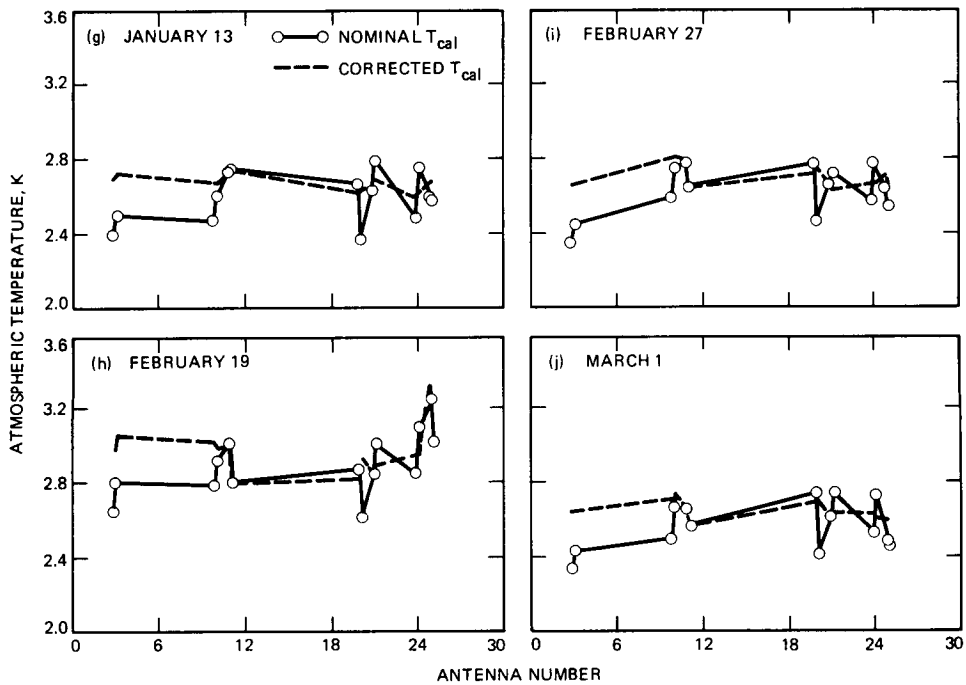
(g) JANUARY 13
NOMINAL T_{cal}
CORRECTED T_{cal}
(i) FEBRUARY 27
(h) FEBRUARY 19
(j) MARCH 1
ATMOSPHERIC TEMPERATURE, K
3.6
3.2
2.8
2.4
2.0
0
6
12
18
24
30
ANTENNA NUMBER

Fig. 3 (contd)

Appendix

Calculation of T_m

An accurate calculation of T_m, the mean radiating temperature of the atmosphere, depends not only on the vertical temperature distribution of the atmosphere at a given time but also on the fact that the two primary molecular contributors (water vapor and oxygen) have different vertical density distributions. Some of the variations observed in T_m from sites within the continental United States are discussed in [8]. For the present purpose we have made use of one year (1976) of radiosonde data from El Paso, Texas, in order to estimate T_m from surface temperature data. El Paso is approximately 280 km from the VLA and is in approximately the same climatic zone, although El Paso is at an altitude of 1200 m versus 2124 m for the VLA site. Using the El Paso data and assuming a linear relation between T_m and the surface temperature T_s gives

$$T_m = 256.9 + 0.445 T_s \qquad \text{(A-1)}$$

where T_s is in degrees Celsius. Note that the sensitivity of T_{atm} with respect to changes in T_m for $\tau_0 \ll 1$ is

$$\frac{dT_{\text{atm}}}{dT_m} = \tau_0 \qquad \text{(A-2)}$$

or

$$\frac{dT_{\text{atm}}}{dT_s} = 0.445\, \tau_0 \qquad \text{(A-3)}$$

For the interval spanned by the data in this article, the zenith opacities are on the order of 0.01 and the surface temperatures vary by roughly 25°C. Hence, we would expect less than 0.1 K variation in T_{atm} from variations in T_m.